RSC Advances

PAPER

View Article Online
View Journal | View Issue

Cite this: *RSC Adv.*, 2022, **12**, 16342

Synthesis and application of novel urea–benzoic acid functionalized magnetic nanoparticles for the synthesis of 2,3-disubstituted thiazolidin-4-ones and hexahydroquinolines†

Fazlulhaq Fazl, Morteza Torabi, Meysam Yarie * and Mohammad Ali Zolfigol

In this work, we reported the synthesis and application of a new urea–benzoic acid containing ligand [$(OEt)_3Si(CH_2)_3$–urea–benzoic acid] for the functionalization of silica coated magnetic nanoparticles. The resulting structure, namely Fe_3O_4@SiO_2@$(CH_2)_3$–urea–benzoic acid, was characterized through different techniques including FT-IR, SEM, EDX-Mapping, VSM and TGA/DTG analysis. Then, Fe_3O_4@SiO_2@$(CH_2)_3$–urea–benzoic acid was applied as a heterogeneous dual acidic and hydrogen bonding catalyst for the synthesis of 2,3-disubstituted thiazolidin-4-ones and hexahydroquinolines under mild and green reaction conditions. More importantly, all of the desired products were obtained with relatively good yields. Also, the catalyst was recovered and reused for four successive runs without significant reduction in yield of the model reaction.

Received 5th April 2022
Accepted 24th May 2022

DOI: 10.1039/d2ra02205b

rsc.li/rsc-advances

Introduction

Since the first introduction of hydrogen bond interactions by Pauling, they have been a subject of extensive research in modern science and technology.[1,2] Moreover, hydrogen bond interactions govern many intermolecular and intramolecular interactions.[3,4] The reason behind the special behaviours of numerous molecules in biological systems can be explained by hydrogen bonding phenomenon.[5] Hydrogen bond interactions have prominent role in numerous relevant areas of chemistry such as enzymatic catalysis,[6] supramolecular chemistry,[7] materials technology,[8] crystal engineering[9] and proton transfer reactions.[10] Meanwhile, hydrogen bond-based organocatalysis has been increasingly promoted by chemists. In this regard, (thio)-ureas, squaramides, phosphoric acid derivatives and guanidines can be used as donor of hydrogen bonding.[11] Recently, hydrogen bonding catalysis manners have been applied in many catalytic organic reactions such as Friedel–Crafts,[12] Mannich,[13] Diels–Alder[14] and multicomponent reactions.[15] Urea and its derivatives as the extraordinary kinds of hydrogen bonding catalysts have potentials of both acidic and basic catalyst and can be coupled with metals.[16,17] Therefore, urea derivatives can be acts as biological catalysts in many of organic reactions.[18]

Due to rapid development of the heterogeneous catalysts as well as their significant benefits, magnetically recoverable solid acids as versatile and sustainable alternatives to homogeneous acids become a considerable research area.[19–22] Magnetically recoverable solid acids due to their unique advantages such as high thermal and chemical stability, chemical tunability, easy recovering and reusability, low toxicity, and high surface area have been emerged the attention of many of technologic and scientific researchers.[23–26] According to high dispersibility of magnetic nanoparticles in solvent and their small size, these materials have been converted to active catalysts in reaction media. In other words, magnetic catalysts are a bridge between heterogeneous and homogeneous catalytic systems.[27] Because of its relative high activity and stability, carboxylic acid functional group is an ideal active site for modification of magnetic nanoparticles (MNPs). Indeed, carboxylic acid and urea functionalized MNPs can provide a suitable heterogeneous catalyst for promoting many of organic reactions.[28,29] Moreover, the existence of both urea and carboxylic acid within a single catalytic system enhances its capabilities in chemical processes.[30]

Chemical methods based on multicomponent synthetic strategy provide a forceful and rapid synthetic route for the synthesis of diverse compounds.[31] Multicomponent synthetic methods have promising approaches due to their unique merits such as high atom economy, available starting materials, efficiency of the protocol, selectivity and facility in the synthesis of complex molecules. Especially, due to ease of work, good efficiency, high atom and step economy and selectivity, catalytic

Department of Organic Chemistry, Faculty of Chemistry, Bu-Ali Sina University, Hamedan, Iran. E-mail: myarie.5266@gmail.com; M.yarie92@basu.ac.ir

† Electronic supplementary information (ESI) available. See https://doi.org/10.1039/d2ra02205b

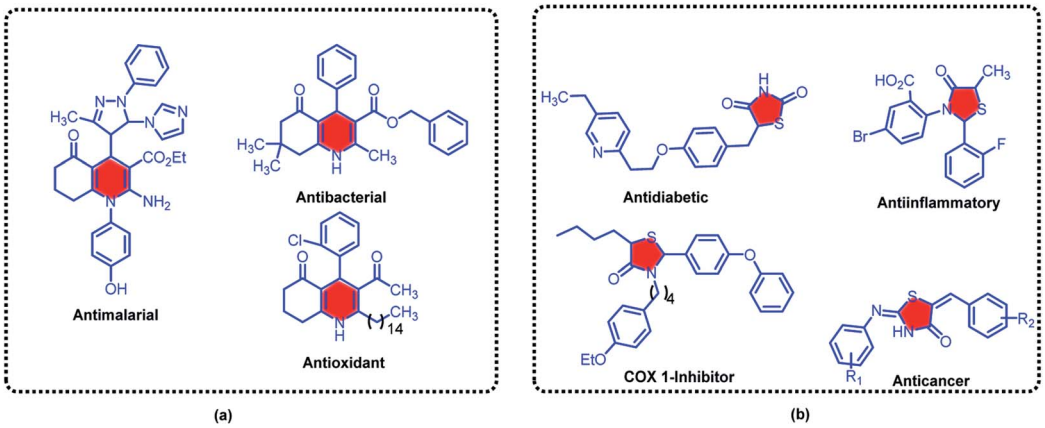

Scheme 1 Some of biologically active examples of hexahydroquinolines (a) thiazolidine bearing molecules (b).

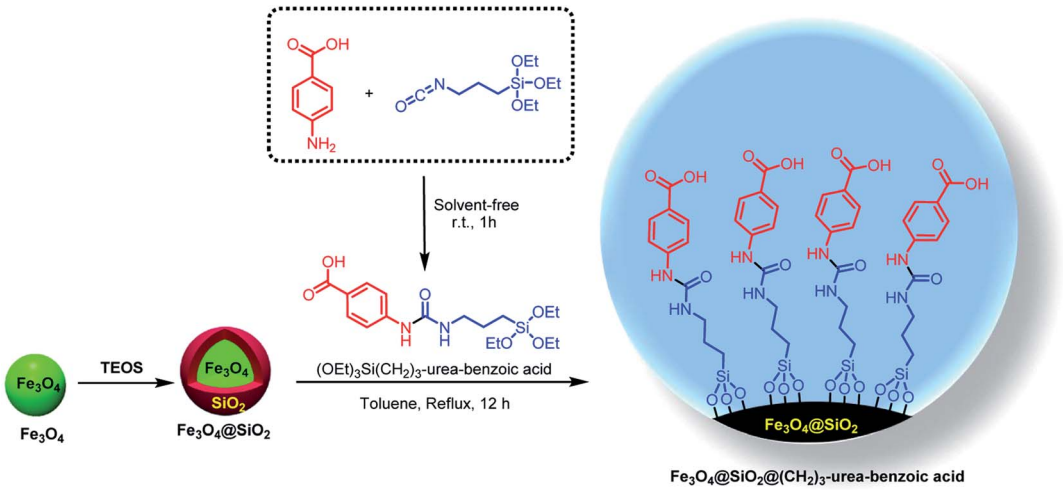

Scheme 2 Representation of the synthetic route of Fe_3O_4@SiO_2@$(CH_2)_3$–urea–benzoic acid.

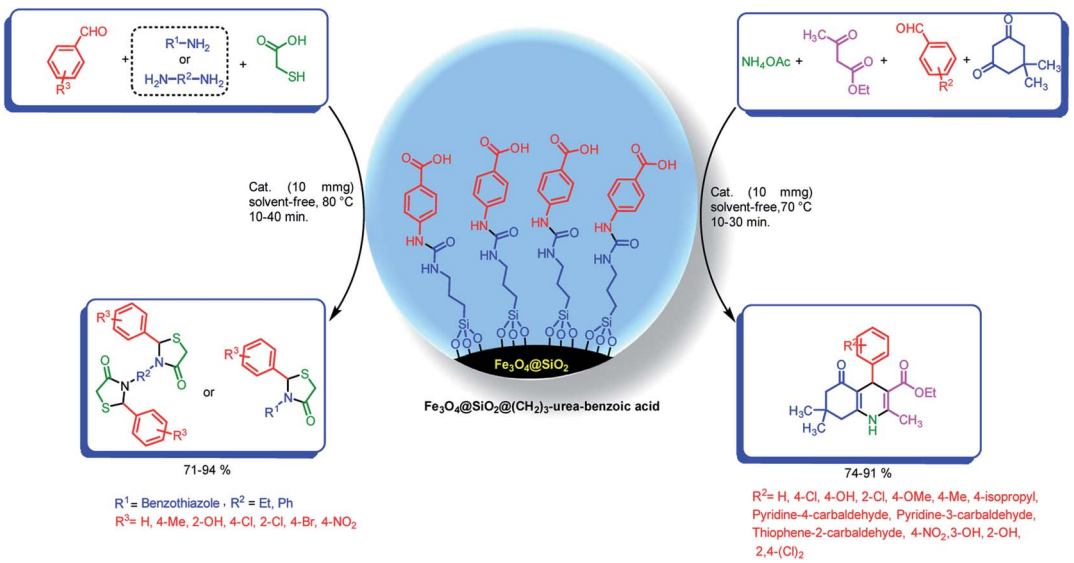

Scheme 3 Preparation of hexahydroquinolines and 2,3-disubstituted thiazolidin-4-ones by using Fe_3O_4@SiO_2@$(CH_2)_3$–urea–benzoic acid as catalyst.

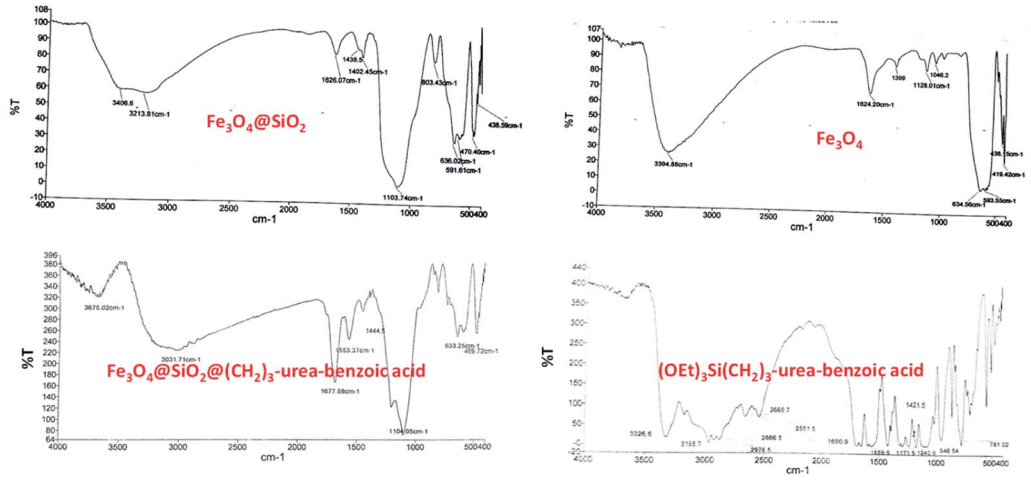

Fig. 1 FT-IR spectra of Fe_3O_4@SiO_2@$(CH_2)_3$–urea–benzoic acid and its related intermediates.

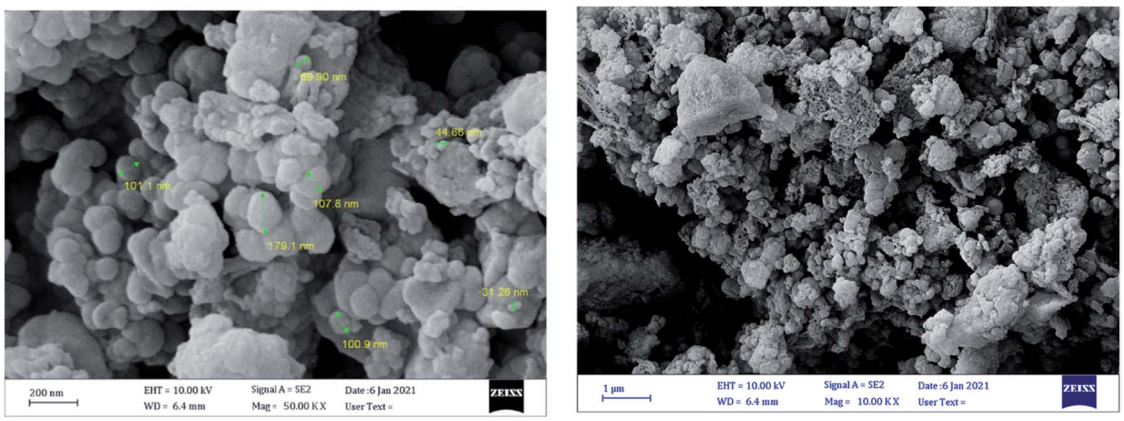

Fig. 2 SEM image of Fe_3O_4@SiO_2@$(CH_2)_3$–urea–benzoic acid.

applications of functionalized magnetic nanoparticles in multicomponent reactions have been noticed by chemists.[32,33]

1,4-Dihydropyridine derivatives which are widely found in natural products represent exceptional pharmacological activities, and therefore received considerable attention in synthetic chemistry.[34–36] Hexahydroquinolines as one of the main important family of 1,4-dihydropyridines, have been studied profoundly.[37–39] Several critical biological applications

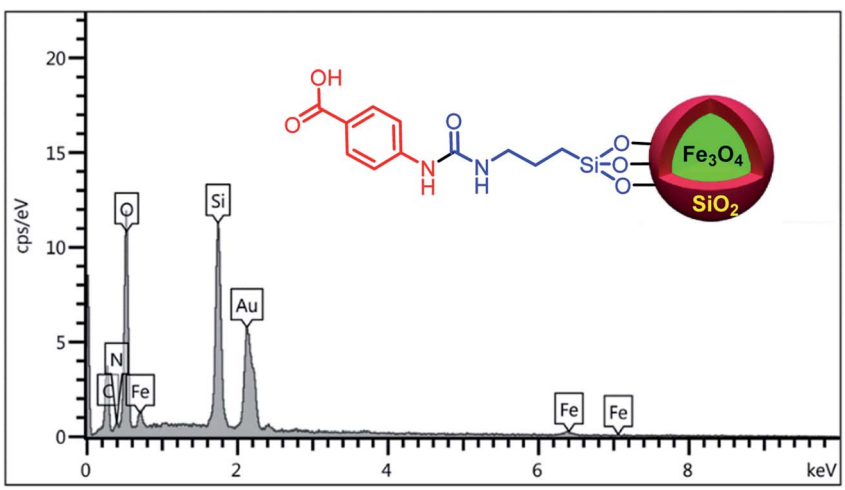

Fig. 3 EDX analysis of Fe_3O_4@SiO_2@$(CH_2)_3$–urea–benzoic acid.

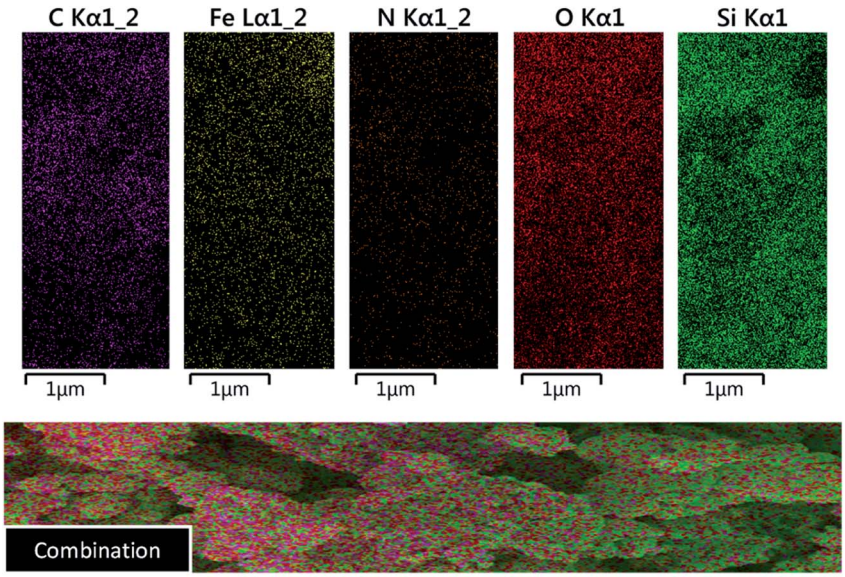

Fig. 4 Displaying the scattering of elements in Fe_3O_4@SiO_2@$(CH_2)_3$–urea–benzoic acid.

and therapeutic activities such as antiplasmodial,[40] antimalarial,[41] antidiabetic,[42] anticancer,[43] bronchodilator,[44] antiatherosclerotic,[45] vasodilator,[46] antibacterial properties[47] and calcium channel blockers in cardiovascular disease treatment[48] have been devoted for these versatile compounds. The structure of some biologically active hexahydroquinolines derivatives is sketched in the Scheme 1.

Nitrogen/sulfur-containing heterocycles with innumerable advantages in agricultural industry and medicinal chemistry are lucrative molecules for any researchers which are involved.[49–52] In this instance, thiazolidine-4-one derivatives as magic example of sulfur-containing heterocycles, have decisive roles in many functional materials, pharmaceuticals and natural products.[53–56] Alternatively, extensive applications of thiazolidines as antiinflammatory,[57] cardiovascular,[58] anticancer,[59] antimicrobial,[60] antioxidant,[61] antimycobacterial,[62] COX-1 inhibitor[63] and antiviral activities[64] are privileged property of these materials (Scheme 1).

With the light of this background and also our previous investigations in the areas of catalytic applications of magnetic nanoparticles in the preparation of heterocyclic compounds,[18,38,65] we designed and synthesized of Fe_3O_4@SiO_2@$(CH_2)_3$–urea–benzoic acid and applied it as recoverable catalyst for the synthesis of hexahydroquinolines and 2,3-disubstituted thiazolidin-4-ones (Schemes 2 and 3).

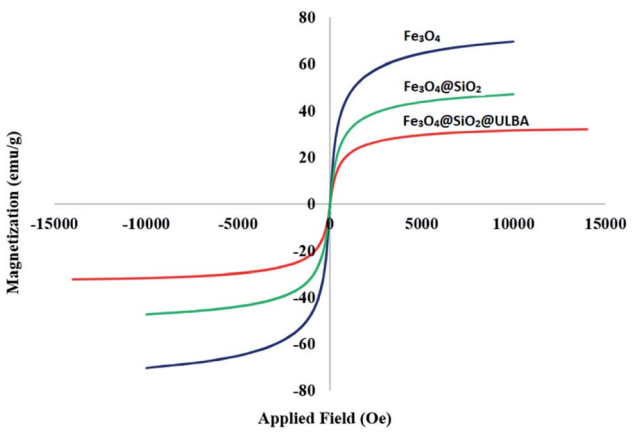

Fig. 5 Comparison of the results of VSM analysis for Fe_3O_4@SiO_2@$(CH_2)_3$–urea–benzoic acid and its related intermediates.

Results and discussion

Since that hydrogen bonding catalyst are great demand and due to our experiences in the synthesis and application of urea containing catalysts,[15,66] it was decided to investigate the obtained results from various characterization techniques from the structure, morphology and physical properties of Fe_3O_4@SiO_2@$(CH_2)_3$–urea–benzoic acid in details.

Firstly, FT-IR technique was applied for characterization of the Fe_3O_4@SiO_2@$(CH_2)_3$–urea–benzoic acid and its related intermediates. In FT-IR spectrum of Fe_3O_4, the broad peak about 3394 cm^{-1} is related to OH groups in the surface of Fe_3O_4 and the significant peak of Fe–O bond is appeared at 634 cm^{-1}. In FT-IR spectrum of Fe_3O_4@SiO_2, the diagnostic peak of Si–O–Si is well shown in 1104 cm^{-1}. According to FT-IR spectrum of $(OEt)_3Si(CH_2)_3$–urea–benzoic acid, the stretching vibration of NH of urea is appeared in 3326 cm^{-1} and the broad acidic peak of benzoic acid is shown in the range of 2669–3326 cm^{-1}. Moreover, high intensity peaks in 1690 and 1559 cm^{-1} confirm the presence of C=O and C=C groups. Finally, in FT-IR spectrum of Fe_3O_4@SiO_2@$(CH_2)_3$–urea–benzoic acid, the observed changes in comparison to previous steps and presence of significant peak at 1677 cm^{-1} and existence of acidic broad peak in the range of 2500–3500 cm^{-1} confirm the successful synthesis of the described catalyst (Fig. 1).

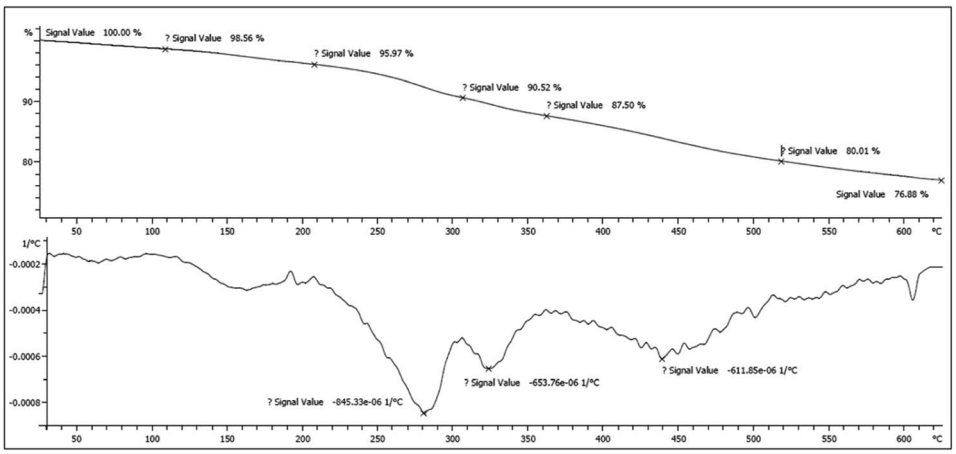

Fig. 6 TGA/DTG analysis of Fe_3O_4@SiO_2@$(CH_2)_3$–urea–benzoic acid.

Scanning electron microscopy (SEM) images were applied for investigation of the morphology and size of the catalyst. As these images show (Fig. 2), the catalyst has spherical morphology and the sizes of catalyst are in the range of 31–179 nm.

In order to confirm the existence of the expected elements including Fe, Si, C, N and O, energy-dispersive X-ray spectroscopy (EDX) analysis was used. According to the observed results, all of mentioned awaited elements are verified (Fig. 3). Also, elemental mapping analysis was applied to confirm the EDX analysis and indicating of particle dispersion (Fig. 4).

In another study, VSM analysis was applied for investigation of magnetic properties of Fe_3O_4@SiO_2@$(CH_2)_3$–urea–benzoic acid and its related intermediates. The results show an order decrease of magnetic properties from Fe_3O_4 to the target catalyst. This well confirms the addition of organic layers onto the surface of Fe_3O_4 (Fig. 5). Also, the amount of saturation of the Fe_3O_4@SiO_2@$(CH_2)_3$–urea–benzoic acid (about of 25 emu g^{-1}) helps to easily separate the catalyst from the reaction mixture.

Achieved data form thermogravimetric and differential thermogravimetric analysis (TGA/DTG) displayed that Fe_3O_4@SiO_2@$(CH_2)_3$–urea–benzoic acid was stable up to 280 °C under

Table 1 Optimizing of the reaction conditions for the synthesis of **1b**[a]

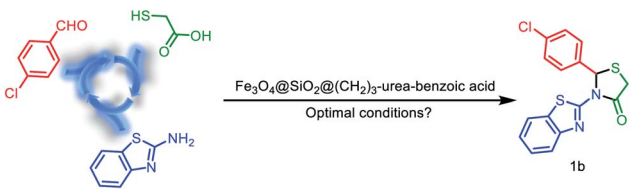

Entry	Solvent	Temperature (°C)	Catalyst loading (mg)	Time (min)	Yield[b] (%)
1	—	90	10	15	88
2	—	80	15	15	87
3[c]	—	**80**	**10**	**15**	**85**
4		80	5	30	72
5	—	80	—	15	Trace
6	—	80	7	15	75
7	—	80	20	15	87
8	—	80	—	120	50
9	—	70	10	30	70
10	—	60	10	100	56
11	H_2O	Reflux	10	60	—
12	EtOH	Reflux	10	60	66
13	*n*-Hexane	Reflux	10	60	40
14	EtOAc	Reflux	10	60	—
15	CH_2Cl_2	Reflux	10	60	—

[a] Reaction conditions: 4-cholorobenzaldehyde (1 mmol, 0.140 g), benzo[*d*]thiazol-2-amine (1 mmol, 0.150 g) and 2-mercaptoacetic acid (1 mmol, 0.092 g). [b] Related to isolated yields. [c] Optimal data.

Table 2 Optimizing of the reaction conditions for the synthesis of **2h**[a]

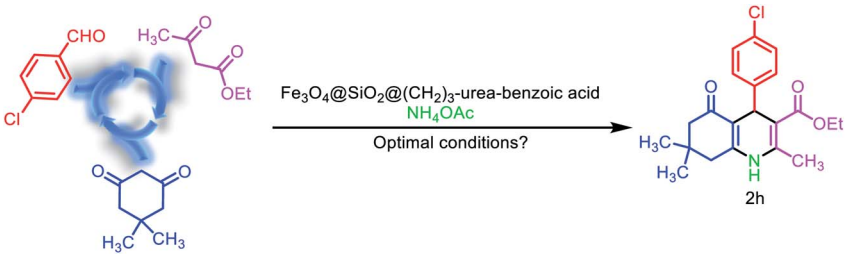

Entry	Solvent	Temperature (°C)	Catalyst loading (mg)	Time (min)	Yield[b] (%)
1	—	90	10	10	92
2	—	80	15	10	90
3[c]	—	**70**	**10**	**10**	**91**
4		70	5	30	80
5	—	70	—	10	Trace
6	—	70	7	10	82
7	—	70	20	10	92
8	—	70	—	120	60
9	—	60	10	30	70
10	—	50	10	100	20
11	H_2O	Reflux	10	60	—
12	EtOH	Reflux	10	60	45
13	*n*-Hexane	Reflux	10	60	—
14	EtOAc	Reflux	10	60	50
15	CH_2Cl_2	Reflux	10	60	—

[a] Reaction conditions: 4-cholorobenzaldehyde (1 mmol, 0.140 g), 5,5-dimethylcyclohexane-1,3-dione (1 mmol, 0.140), ethyl acetoacetate (1 mmol, 0.130 g), ammonium acetate (1 mmol, 0.078 g). [b] Related to isolated yields. [c] Optimal data.

N_2 atmosphere (Fig. 6). The slight weight loss in the range of 100–150 °C is related to the removal of trapped solvents and the major weight loss in 280 °C was attributed to destruction of organic layers. A total weight loss up to 23% indicates that a significant amount of the catalyst contained organic layers.

After the characterization of Fe_3O_4@SiO_2@$(CH_2)_3$–urea–benzoic acid, we investigated and optimized various reaction parameters such as solvent, temperature and amount of catalyst for the synthesis of 2,3-disubstituted thiazolidin-4-ones. The model reaction was carried out *via* one-pot three component condensation reaction between of 4-chloro benzaldehyde, benzo[*d*]thiazol-2-amine and 2-mercaptoacetic acid. At first, different temperatures such as 90, 80, 70 and 60 °C were applied for the model reaction. According to results, 80 °C was selected as optimized temperature. After that, several amounts of catalyst were used. The results indicate that the 10 mg of catalyst is the best amount. Finally, the role of solvent for the model reaction were explored. For this purpose, the reactions were performed under solvent-free conditions and in various protic and aprotic solvents. The results showed that the solvent-free conditions have the best yield (Table 1). Also, the obtained results from the optimizing of the reaction conditions for the synthesis of molecule **2h** (as model reaction for the preparation of hexahydroquinolines) are embedded in Table 2. The results indicating that best data were achieved under the solvent free conditions at 70 °C in the presence of 10 mg of catalyst (entry 3).

Under the optimized reaction conditions (10 mg of Fe_3O_4@SiO_2@$(CH_2)_3$–urea–benzoic acid as catalyst and solvent-free conditions at 80 °C) the substrate scope for the general validity of 2,3-disubstituted thiazolidin-4-ones and hexahydroquinolines was explored. Hereupon, assortment of aromatic aldehydes with electron-poor and electron-rich aryl groups, aromatic and aliphatic amines and 2-mercaptoacetic acid were applied for the synthesis of 2,3-disubstituted thiazolidin-4-one derivatives (Table 3). Likewise, variety of aromatic aldehydes with electron-poor and electron-rich aryl groups, ethyl acetoacetate, 5,5-dimethylcyclohexane-1,3-dione and ammonium acetate were used for the synthesis of hexahydroquinoline derivatives (Table 4).

Due to privileged character of magnetic nanoparticles in recycling and reusing, we investigated the recoverability of Fe_3O_4@SiO_2@$(CH_2)_3$–urea–benzoic acid in the model reaction. After running and completing each of the reactions, the resulting mixture was dissolved in 10 mL of hot ethanol and catalyst was separated from the mixture of reaction by using an external magnet. It was washed three times with ethanol. After that, the recovered catalyst was desiccated under air conditions. This process was repeated for four times without significant reduction in efficiency (Fig. 7).

In a separate study, according to suggested mechanism for the synthesis of 2,3-disubstituted thiazolidin-4-ones (Scheme 5), in the presence of catalyst, the carbonyl group of benzaldehyde

Table 3 Synthesis of 2,3-disubstituted thiazolidin-4-ones in the presence of Fe_3O_4@SiO_2@$(CH_2)_3$–urea–benzoic acid as catalyst[a]

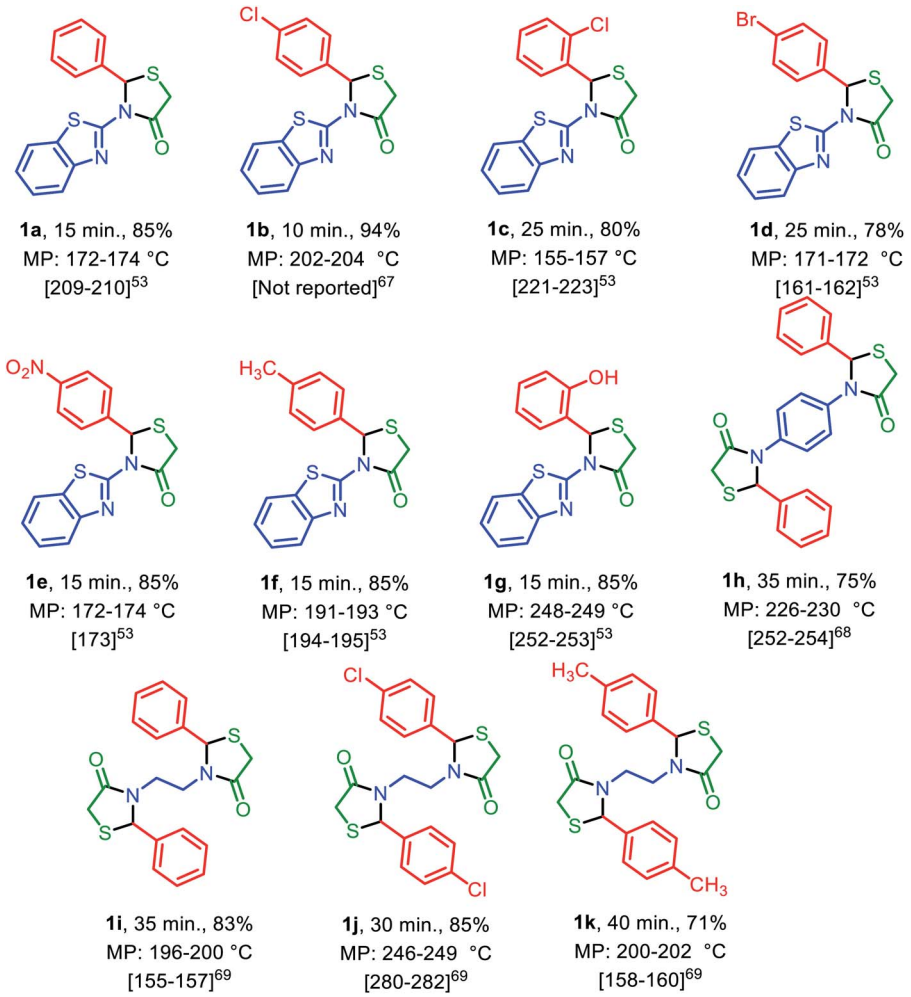

[a] Reaction conditions: arylaldehyde (2 mmol), amine (2 or 1 mmol) and 2-mercaptoacetic acid (2 mmol, 0.184 g), solvent-free, 80 °C, catalyst = 10 mg, reported yields are referred to isolated yields.

was activated and reacted with benzo[*d*]thiazol-2-amine which leads to formation of intermediate **a**. In the second step, *via* the reaction of intermediate **a** with 2-mercaptoacetic acid, the intermediate **b** was formed. Finally, due to nucleophilic intermolecular cyclization and removing of H_2O, the desired product **1a** was obtained (Scheme 4).

Also, we suggested a plausible mechanism for the synthesis of hexahydroquinolines and 2,3-disubstituted thiazolidin-4-ones. According to sketched mechanism for the synthesis of hexahydroquinolines (Scheme 5), the carbonyl group of benzaldehyde was activated by catalyst and undergoes a nucleophilic attack from the enol form of 5,5-dimethylcyclohexane-1,3-dione. This reaction leads to formation of Knoevenagel adduct **d**. Also, the released ammonia from thermal dissociation of ammonium acetate was reacted with ethyl acetoacetate and intermediate **e** was formed. In the next step, through the reaction between of intermediates **d** and **e**, the intermediate **f** was performed. After that, through a tautomerization process and nucleophilic intermolecular cyclization, the intermediate **h** was obtained. Then, through removing of H_2O, the target product **2a** was performed. It is worthy to mention that, authors believed that due to the strong resonance interaction between lone pair electrons of nitrogen atom with two carbonyl groups as strong acceptors. Therefore, there is no effectual interaction between lone pair electrons of nitrogen and σ* orbital of sp^3 C–H bond. Herein, anomeric effect was not occurred.[72] Thus, vinylogous anomeric-based oxidation[72] is not effective alone for the oxidation of hexahydroquinolines to their corresponding aromatized pyridines.

Experimental

General experimental procedure for the synthesis of Fe_3O_4@SiO_2@$(CH_2)_3$–urea–benzoic acid

Initially, into a 10 mL round-bottomed flask containing 4-amino-benzoic acid (5 mmol, 0.686 g), 3-isocyanatopropyltriethoxysilane (5 mmol, 2.237 g) was added and then the resulting mixture was stirred for **1h** under solvent-free

Table 4 Synthesis of hexahydroquinolines in the presence of Fe_3O_4@SiO_2@$(CH_2)_3$–urea–benzoic acid as catalyst[a]

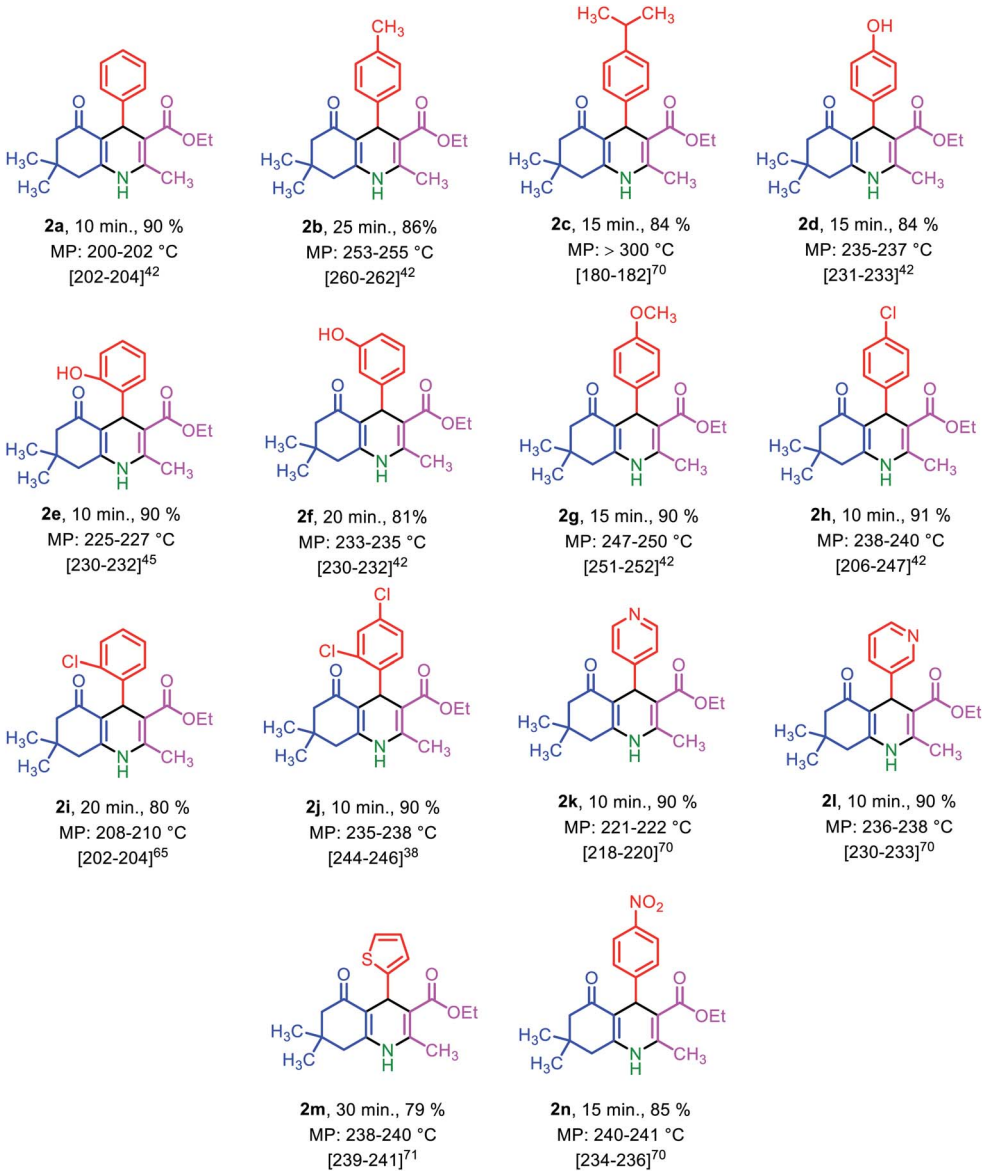

[a] Reaction conditions: arylaldehyde (1 mmol), 5,5-dimethylcyclohexane-1,3-dione (1 mmol, 0.140), ethyl acetoacetate (1 mmol, 0.130 g), ammonium acetate (1 mmol, 0.078 g), solvent-free, 70 °C, catalyst = 10 mg, reported yields are referred to isolated yields.

conditions at room temperature. After completing of the reaction, the precipitate was washed and purified by *n*-hexane/dichloromethane (3 : 10) and dried at room temperature in a short time to give $(OEt)_3Si(CH_2)_3$–urea–benzoic acid (yield: 92%). Then, Fe_3O_4 and Fe_3O_4@SiO_2 was synthesized according to our reported procedure.[18a] After that, into a 100 mL round-bottomed flask, Fe_3O_4@SiO_2 (1.0 g) and $(OEt)_3Si(CH_2)_3$–urea–benzoic acid (2.0 mmol, 0.768 g) were added and the reaction was proceeded under toluene reflux for 12 hours to give Fe_3O_4@SiO_2@$(CH_2)_3$–urea–benzoic acid. Then, final product was separated with external magnet and washed with *n*-hexane (50 mL) and EtOH (20 mL) and dried in air conditions.

Experimental route for the preparation of 2,3-disubstituted thiazolidin-4-ones

To the mixture of aldehyde derivatives (2 mmol), amine derivatives (2 mmol for 2-aminobenzothiazole and 1 mmol for ethylene diamine or phenylene diamine), 2-mercaptoacetic acid (2 mmol, 0.184 g) in a 10 mL round-bottomed flask, 0.01 g of Fe_3O_4@SiO_2@$(CH_2)_3$–urea–benzoic acid as catalyst was added. The mixture of reaction was placed in an oil bath and stirred under solvent-free conditions at 80 °C. The progress of the reaction was monitored by TLC technique (ethyl acetate/*n*-hexane as eluent, 1 : 1). After completing of the reaction, 10 mL of hot EtOH was added to the reaction mixture. After dissolving all of materials in EtOH except catalyst, the catalyst was

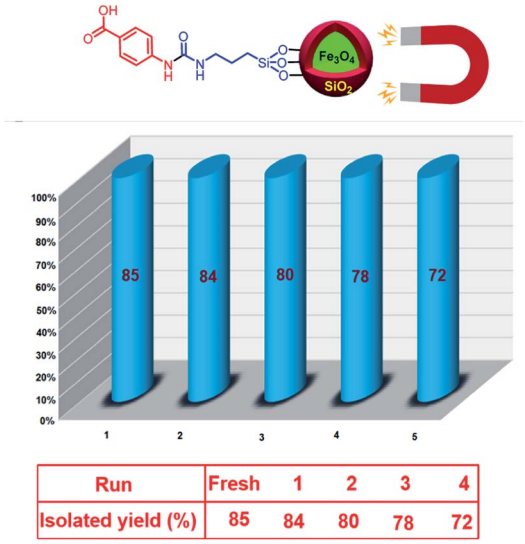

Run	Fresh	1	2	3	4
Isolated yield (%)	85	84	80	78	72

Fig. 7 Recovering test of Fe_3O_4@SiO_2@$(CH_2)_3$–urea–benzoic acid in the synthesis of **1b**.

separated from the mixture of reaction by an external magnet. Finally, the desired products were washed with EtOH and desiccated at 80 °C to obtain a pure solid.

Experimental procedure for the preparation of hexahydroquinolines

Into a 10 mL round-bottomed flask, 5,5-dimethylcyclohexane-3,1-dione (1 mmol, 0.14 g), aromatic aldehyde (1 mmol), ethyl acetoacetate (1 mmol, 0.13 g), ammonium acetate (1 mmol, 0.078) and 0.01 g of Fe_3O_4@SiO_2@$(CH_2)_3$–urea–benzoic acid as catalyst were added. The mixture of reaction was then stirred under solvent-free conditions at 80 °C. The progress of the reaction was evaluated using the TLC technique (ethyl acetate/*n*-hexane as eluent, 1 : 1). After completing of the reaction, 10 mL of hot EtOH was added to the reaction mixture. All materials except catalyst was completely dissolved and catalyst was removed from the mixture of reaction by an external magnet. Finally, the desired products were washed with EtOH and dried at 80 °C to obtain a pure solid.

Selected spectral data

$(OEt)_3Si(CH_2)_3$–urea–benzoic acid. M. p.: 276–278 °C, FT-IR (KBr, ν, cm^{-1}): 3326, 3188, 2978, 1690, 1559, 1171. ^{1}H NMR (301 MHz, DMSO) δ 12.49 (s, 1H), 8.80 (s, 1H), 7.84 (d, J = 9 Hz, 2H), 7.52 (d, J = 9 Hz, 2H), 6.33 (t, J = 6 Hz, 1H), 3.75 (q, J = 7 Hz, 6H), 3.10 (q, J = 6.6 Hz, 2H), 1.51 (p, J = 7.7 Hz, 2H), 1.16 (t, J = 7 Hz, 9H), 0.57 (t, J = 9 Hz, 2H). ^{13}C NMR (76 MHz, DMSO) δ 167.6, 155.2, 145.4, 130.9, 123.2, 117.0, 58.2, 42.2, 23.7, 18.6, 7.7.

3-(Benzo[*d*]thiazol-2-yl)-2-phenylthiazolidin-4-one (1a). M.p. = 172–174 °C, FT-IR (KBr, ν, cm^{-1}): 3067, 1696, 1573, 1504, 1441, 1373, 1270. ^{1}H NMR (301 MHz, DMSO) δ 8.03 (d, J = 9 Hz, 1H), 7.67 (d, J = 9 Hz, 1H), 7.40–7.27 (m, 7H), 6.93 (s, 1H), 4.30 (d, J = 15 Hz, 1H), 4.04 (d, J = 18 Hz, 1H). ^{13}C NMR (76 MHz, DMSO) δ 172.2, 156.5, 148.1, 141.6, 131.5, 129.2, 128.5, 126.9, 125.9, 124.9, 122.4, 121.8, 63.2, 32.4.

3-(Benzo[*d*]thiazol-2-yl)-2-(4-chlorophenyl)thiazolidin-4-one (1b). M.p. = 202–204 °C, FT-IR (KBr, ν, cm^{-1}): 3060, 1693, 1594, 1367, 1498, 1280. ^{1}H NMR (301 MHz, DMSO) δ 8.04 (d, J = 6 Hz, 1H), 7.69 (d, J = 9 Hz, 1H), 7.49–7.33 (m, 6H), 6.94 (s, 1H), 4.33 (d, J = 15 Hz, 1H), 4.06 (d, J = 15 Hz, 1H). ^{13}C NMR (76 MHz, DMSO) δ 172.1, 156.5, 148.1, 140.7, 133.0, 131.8, 129.2, 128.0, 126.9, 124.9, 122.5, 121.8, 62.6, 32.3.

3-(Benzo[*d*]thiazol-2-yl)-2-(2-chlorophenyl)thiazolidin-4-one (1c). M.p. = 155–157 °C, FT-IR (KBr, ν, cm^{-1}): 3386, 3061, 1705, 1590, 1444, 1276, 1050. ^{1}H NMR (301 MHz, DMSO) δ 8.07 (d, J = 6 Hz, 1H), 7.68 (d, J = 9 Hz, 1H), 7.59 (d, J = 6 Hz, 1H), 7.44–7.26 (m, 4H), 7.14 (d, J = 6 Hz, 1H), 7.00 (s, 1H), 4.23 (d, J = 18 Hz, 1H), 4.10 (d, J = 15 Hz, 1H). ^{13}C NMR (76 MHz, DMSO) δ 172.3, 156.4, 148.1, 137.9, 131.8, 131.6, 130.6, 130.2, 128.3, 126.9, 125.6, 125.0, 122.5, 121.9, 60.8, 32.1.

3,3′-(Ethane-1,2-diyl)bis(2-phenylthiazolidin-4-one) (1f). M.p. = 196–200 °C, FT-IR (KBr, ν, cm^{-1}): 3034, 1662, 1450, 1430, 1270, 1153. ^{1}H NMR (301 MHz, DMSO) δ 7.39–7.30 (m, 10H), 5.70 (s, 2H), 3.84 (d, J = 15 Hz, 2H), 3.64 (d, J = 15 Hz, 2H), 3.55 (dd, J = 12, J = 6, 2H), 2.67 (dd, J = 15, J = 6, 2H). ^{13}C NMR (76 MHz, DMSO) δ 171.4, 140.3, 129.4, 129.3, 127.5, 62.9, 32.2.

3,3′-(Ethane-1,2-diyl)bis(2-(4-methylphenyl)thiazolidin-4-one) (1h). M.p. = 200–202 °C, FT-IR (KBr, ν, cm^{-1}): 3324, 2999, 1668, 1573, 1407, 1266. ^{1}H NMR (301 MHz, DMSO) δ 7.21–7.15 (m, 8H), 5.64 (s, 2H), 3.81 (dd, J = 15, 3 Hz, 2H), 3.62 (d, J = 15 Hz, 2H), 3.50 (dd, J = 15, 6 Hz, 2H), 2.61 (dd, J = 15, J = 6, 2H). ^{13}C NMR (76 MHz, DMSO) δ 171.3, 138.7, 137.2, 129.9, 127.5, 62.8, 32.2, 21.3.

Ethyl 2,7,7-trimethyl-5-oxo-4-phenyl-1,4,5,6,7,8-hexahydroquinoline-3-carboxylate (2a). M.p. = 200–202 °C, FT-IR (KBr, ν, cm^{-1}): 3275, 3076, 2961, 1699, 1604, 1489, 1213.

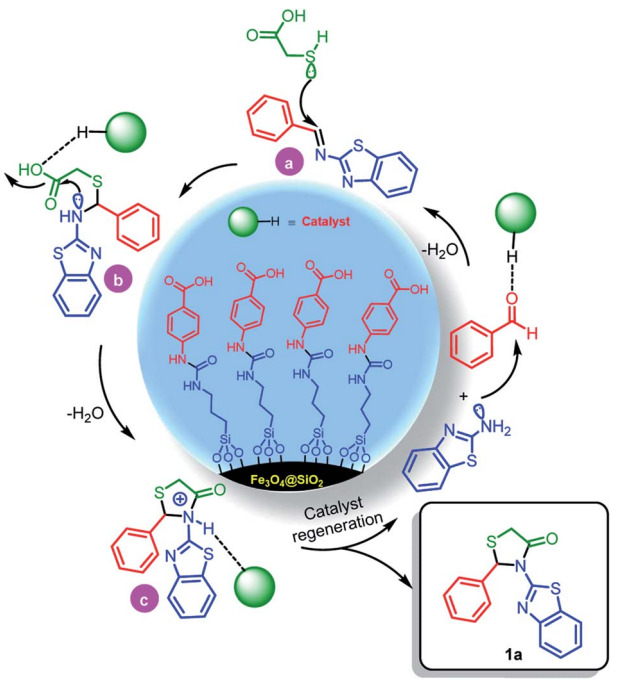

Scheme 4 The suggested mechanism for the synthesis of **1a** in the presence of Fe_3O_4@SiO_2@$(CH_2)_3$–urea–benzoic acid as catalyst.

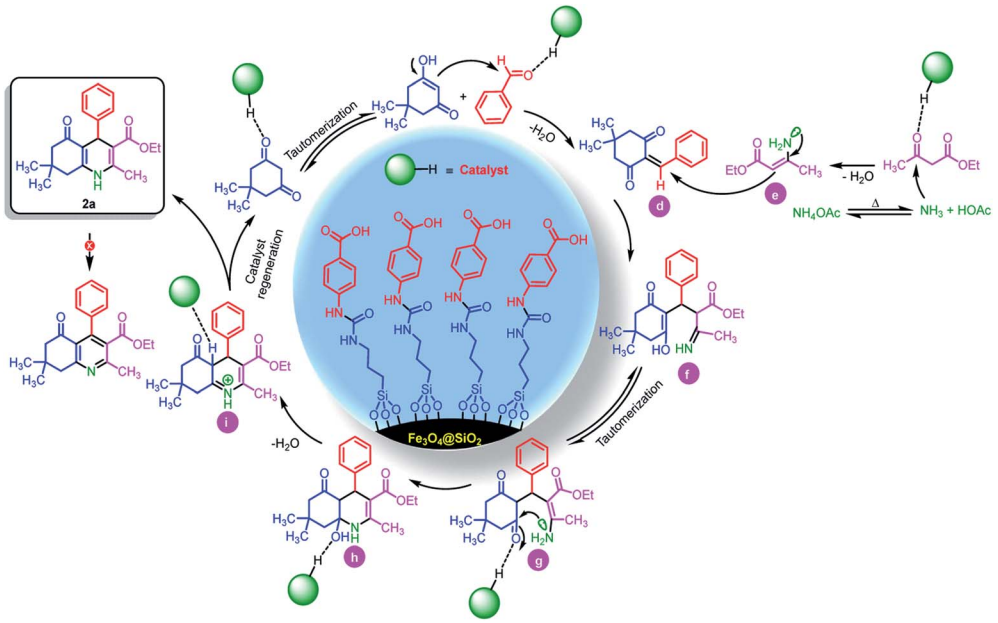

Scheme 5 The plausible mechanism for the synthesis of **2a** in the presence of Fe_3O_4@SiO_2@$(CH_2)_3$–urea–benzoic acid as catalyst.

^{1}H NMR (301 MHz, DMSO) δ 9.11 (s, 1H, NH), 7.22–7.06 (m, 5H, Aromatic), 4.88 (s, 1H, CH), 3.99 (q, J = 7.0 Hz, 2H, CH_2), 2.47–2.31 (m, 1H), 2.19 (d, J = 15, 1H), 1.99 (d, J = 15, 1H), 1.14 (t, J = 7 Hz, 3H), 1.02–0.98 (m, 3H), 0.86 (s, 3H). ^{13}C NMR (76 MHz, DMSO) δ 194.7, 167.3, 150.0, 148.1, 145.5, 128.2, 127.9, 126.2, 110.5, 104.1, 59.5, 50.7, 36.3, 32.6, 29.6, 26.9, 18.8, 14.6.

Ethyl 4-(4-methoxyphenyl)-2,7,7-trimethyl-5-oxo-1,4,5,6,7,8-hexahydroquinoline-3-carboxylate (2f). M.p. = 247–250 °C, FT-IR (KBr, ν, cm^{-1}): 3276, 3078, 2957, 1701, 1605, 1508, 1380. ^{1}H NMR (301 MHz, DMSO) δ 9.04 (s, 1H), 7.08 (d, J = 6 Hz, 2H, aromatic), 6.76 (d, J = 6 Hz, 2H, aromatic), 4.82 (s, 1H, CH), 4.0 (q, J = 7 Hz, 2H, CH_2), 3.69 (s, 3H, OCH_3), 2.53–2.30 (m, 5H), 2.19 (d, J = 15 Hz, 1H), 1.99 (d, J = 15 Hz, 1H), 1.16 (t, J = 7.1 Hz, 3H), 1.03 (s, 3H), 0.88 (s, 3H). ^{13}C NMR (76 MHz, DMSO) δ 194.8, 167.4, 157.8, 149.7, 145.1, 140.5, 128.9, 113.6, 110.7, 104.4, 59.5, 55.3, 50.8, 35.4, 32.6, 29.6, 27.0, 18.8, 14.7.

Ethyl 4-(4-methoxyphenyl)-2,7,7-trimethyl-5-oxo-1,4,5,6,7,8-hexahydroquinoline-3-carboxylate (2g). M.p. = 238–240 °C, FT-IR (KBr, ν, cm^{-1}): 3293, 3083, 2958, 1667, 1612, 1487, 1217. ^{1}H NMR (301 MHz, DMSO) δ 8.90 (s, 1H, NH), 7.04–6.93 (m, 4H, aromatic), 4.63 (s, 1H, CH), 3.75 (d, J = 6 Hz, 2H, CH_2), 2.23–1.73 (m, 7H), 0.92–0.61 (m, 9H). ^{13}C NMR (76 MHz, DMSO) δ 194.7, 167.1, 150.1, 147.1, 145.9, 130.7, 129.8, 128.2, 110.2, 103.6, 59.6, 50.7, 36.1, 32.6, 29.6, 26.9, 18.8, 14.6.

Conclusion

In summary, we have reported concise and significant protocols for the preparation of hexahydroquinolines and 2,3-disubstituted thiazolidin-4-onederivatives using Fe_3O_4@SiO_2@$(CH_2)_3$–urea–benzoic acid as a novel and reusable nanomagnetic catalyst. Furthermore, the described catalyst was characterized by several techniques. By using various amines and aldehydes the broad substrate scope for the general validity of 2,3-disubstituted thiazolidin-4-ones and hexahydroquinolines was investigated. Our method was able to produce a relatively wide range of functionalized thiazolidinones and hexahydroquinolines under mild reaction conditions while products have relatively good yields.

Conflicts of interest

There are no conflicts to declare.

Acknowledgements

We thank the Bu-Ali Sina University and Iran National Science Foundation [(INSF), Grant Number: 98001912] for financial support to our research group.

References

1 S. J. Grabowski, *Chem. Rev.*, 2011, **111**, 2597.
2 A. S. Mahadevi and G. N. Sastry, *Chem. Rev.*, 2016, **116**, 2775.
3 Y. J. Jin, T. Aoki and G. Kwak, *Angew. Chem., Int. Ed.*, 2020, **59**, 1837.
4 I. Helmers, G. Ghosh, R. Q. Albuquerque and G. Fernández, *Angew. Chem., Int. Ed.*, 2021, **60**, 4368.
5 M. S. Taylor and E. N. Jacobsen, *Angew. Chem., Int. Ed.*, 2006, **45**, 1520.
6 R. S. Proctor, A. C. Colgan and R. J. Phipps, *Nat. Chem.*, 2020, **12**, 990.
7 (*a*) F. Zapata, L. Gonzalez, A. Caballero, A. Bastida, D. Bautista and P. Molina, *J. Am. Chem. Soc.*, 2018, **140**, 2041; (*b*) M. Torabi, *Iran. J. Catal.*, 2021, **11**, 199.
8 R. B. Lin, Y. He, P. Li, H. Wang, W. Zhou and B. Chen, *Chem. Soc. Rev.*, 2019, **48**, 1362.

9 S. Saha, M. K. Mishra, C. M. Reddy and G. R. Desiraju, *Acc. Chem. Res.*, 2018, **51**, 2957.
10 Z. Tang, H. Wei and P. Zhou, *J. Mol. Liq.*, 2020, **301**, 112415.
11 M. C. Gimeno and R. P. Herrera, *Eur. J. Org. Chem.*, 2020, **2020**, 1057.
12 M. Hatano, H. Okamoto, T. Kawakami, K. Toh, H. Nakatsuji, A. Sakakura and K. Ishihara, *Chem. Sci.*, 2018, **9**, 6361.
13 T. Nakamura, K. Okuno, R. Nishiyori and S. Shirakawa, *Chem.–Asian J.*, 2020, **15**, 463.
14 P. Vermeeren, T. A. Hamlin, F. M. Bickelhaupt and I. Fernández, *Chem.–Asian J.*, 2021, **27**, 5180.
15 B. Atashkar, M. A. Zolfigol and S. Mallakpour, *Mol. Catal.*, 2018, **452**, 192.
16 C. Zhu, H. Tang, K. Yang, X. Wu, Y. Luo, J. Wang and Y. Li, *Catal. Commun.*, 2020, **135**, 105837.
17 C. M. McGuirk, M. J. Katz, C. L. Stern, A. A. Sarjeant, J. T. Hupp, O. K. Farha and C. A. Mirkin, *J. Am. Chem. Soc.*, 2015, **137**, 919.
18 (*a*) M. Torabi, M. A. Zolfigol, M. Yarie, B. Notash, S. Azizian and M. Mirzaei Azandaryani, *Sci. Rep.*, 2021, **11**, 1; (*b*) M. Torabi, M. Yarie and M. A. Zolfigol, *Appl. Organomet. Chem.*, 2019, **33**, e4933; (*c*) P. Ghasemi, M. Yarie, M. A. Zolfigol, A. A. Taherpour and M. Torabi, *ACS Omega*, 2020, **5**, 3207.
19 A. Wang, P. Sudarsanam, Y. Xu, H. Zhang, H. Li and S. Yang, *Green Chem.*, 2020, **22**, 2977.
20 J. Gardy, A. Osatiashtiani, O. Céspedes, A. Hassanpour, X. Lai, A. F. Lee, K. Wilson and M. Rehan, *Appl. Catal., B*, 2018, **234**, 268.
21 W. Xie and H. Wang, *Fuel*, 2021, **283**, 118893.
22 B. Changmai, A. E. Wheatley, R. Rano, G. Halder, M. Selvaraj, U. Rashid and S. L. Rokhum, *Fuel*, 2021, **305**, 121576.
23 Q. Zhang, X. Yang and J. Guan, *Appl. Catal., B*, 2019, **2**, 4681.
24 A. Sanchez Diaz-Marta, S. Yanez, C. R. Tubio, V. L. Barrio, Y. Pineiro, R. Pedrido, J. Rivas, M. Amorin, F. Guitián and A. Coelho, *ACS Appl. Mater. Interfaces*, 2019, **11**, 25283.
25 F. Matloubi Moghaddam, M. Eslami and G. Hoda, *Sci. Rep.*, 2020, **10**, 1.
26 S. Shylesh, V. Schuenemann and W. R. Thiel, *Angew. Chem., Int. Ed.*, 2010, **49**, 3428.
27 N. Koukabi, E. Kolvari, M. A. Zolfigol, A. Khazaei, B. S. Shaghasemi and B. Fasahati, *Adv. Synth. Catal.*, 2012, **354**, 2001.
28 S. Yu and G. M. Chow, *J. Mater. Chem.*, 2004, **14**, 2781.
29 A. Angelopoulou, A. Kolokithas-Ntoukas, C. Fytas and K. Avgoustakis, *ACS Omega*, 2019, **4**, 22214.
30 C. Min and D. Seidel, *Chem. Soc. Rev.*, 2017, **46**, 5889.
31 B. B. Toure and D. G. Hall, *Chem. Rev.*, 2009, **109**, 4439.
32 A. C. Boukis, K. Reiter, M. Frölich, D. Hofheinz and M. A. Meier, *Nat. Commun.*, 2018, **9**, 4383.
33 Q. Xiong, S. Dong, Y. Chen, X. Liu and X. Feng, *Nat. Commun.*, 2019, **10**, 5029.
34 M. A. Bodaghifard, A. Mobinikhaledi and S. Asadbegi, *Appl. Organomet. Chem.*, 2017, **31**, e3557.
35 J. A. Bull, J. J. Mousseau, G. Pelletier and A. B. Charette, *Chem. Rev.*, 2012, **112**, 2642.
36 A. Heusler, J. Fliege, T. Wagener and F. Glorius, *Angew. Chem., Int. Ed.*, 2021, **60**, 13793.
37 H. Aghahosseini, M. R. Ranjbar and A. Ramazani, *ChemistrySelect*, 2020, **5**, 8415.
38 M. Yarie, M. A. Zolfigol, Y. Bayat, A. Asgari, D. A. Alonso and A. Khoshnood, *RSC Adv.*, 2016, **6**, 82842.
39 R. Farsi, M. K. Mohammadi and S. J. Saghanezhad, *Res. Chem. Intermed.*, 2021, **47**, 1161.
40 B. S. Hote, T. A. Siddiqui and P. M. Pisal, *Polycyclic Aromat. Compd.*, 2021, 1.
41 P. Choudhury, P. Ghosh and B. Basu, *Mol. Divers.*, 2020, **24**, 283.
42 A. Ghorbani-Choghamarani, M. Mohammadi, T. Tamoradi and M. Ghadermazi, *Polyhedron*, 2019, **158**, 25.
43 R. R. Raslan, S. A. Hessein, S. A. Fouad and N. A. Shmiess, *J. Heterocycl. Chem.*, 2021, **59**, 832.
44 A. Ghorbani-Choghamarani, B. Tahmasbi and Z. Moradi, *Appl. Organomet. Chem.*, 2017, **31**, e3665.
45 S. C. Jadhvar, H. M. Kasraliker, S. V. Goswami, A. V. Chakrawar and S. R. Bhusare, *Res. Chem. Intermed.*, 2017, **43**, 7211.
46 A. Ghorbani-Choghamarani, B. Tahmasbi, P. Moradi and N. Havasi, *Appl. Organomet. Chem.*, 2016, **30**, 619.
47 M. Zabihzadeh, A. Omidi, F. Shirini, H. Tajik and M. S. N. Langarudi, *J. Mol. Struct.*, 2020, **1206**, 127730.
48 S. K. Das, S. Mondal, S. Chatterjee and A. Bhaumik, *ChemCatChem*, 2018, **10**, 2488.
49 M. A. Ansari, D. Yadav and M. S. Singh, *J. Org. Chem.*, 2020, **85**, 8320.
50 V. Jaiswal, B. Mondal, K. Singh, D. Das and J. Saha, *Org. lett.*, 2019, **21**, 5848.
51 J. Safaei-Ghomi, S. H. Nazemzadeh and H. Shahbazi-Alavi, *Appl. Organomet. Chem.*, 2016, **30**, 911.
52 N. Azgomi and M. Mokhtary, *J. Mol. Catal. A: Chem.*, 2015, **398**, 58.
53 M. Kalhor and S. Banibairami, *RSC Adv.*, 2020, **10**, 41410.
54 J. Sun, T. Wang, X. Zhu, W. Xu, B. Cheng and H. Zhai, *New J. Chem.*, 2021, **45**, 14508.
55 D. B. Yedage and D. V. Patil, *ChemistrySelect*, 2018, **3**, 3611.
56 (*a*) K. S. S. Kumar, A. Hanumappa, M. Vetrivel, M. Hegde, Y. R. Girish, T. R. Byregowda, S. Rao, S. C. Raghavan and K. S. Rangappa, *Bioorg. Med. Chem. Lett.*, 2015, **25**, 3616; (*b*) K. S. S. Kumar, A. Hanumappa, M. Hegde, K. H. Narasimhamurthy, S. C. Raghavan and K. S. Rangappa, *Eur. J. Med. Chem.*, 2014, **81**, 341; (*c*) K. S. S. Kumar, T. R. Swaroop, K. B. Harsha, K. H. Narasimhamurthy and K. S. Rangappa, *Tetrahedron Lett.*, 2012, **53**, 5619; (*d*) K. H. Narasimhamurthy, S. Chandrappa, K. S. S. Kumar, T. R. Swaroop and K. S. Rangappa, *Chem. Lett.*, 2013, **42**, 1073.
57 A. M. Shawky, M. A. Abourehab, A. N. Abdalla and A. M. Gouda, *Eur. J. Med. Chem.*, 2020, **185**, 111780.
58 G. Wang, S. Zhao, R. Chen, L. Yang, J. Wang, H. Guo, M. Wu, J. Domena, Y. Xing and S. Sun, *Tetrahedron Lett.*, 2017, **58**, 4308.

59 B. Qi, Y. Yang, G. Gong, H. He, X. Yue, X. Xu, Y. Hu, J. Li, T. Chen, X. Wan, A. Zhang and G. Zhou, *Eur. J. Med. Chem.*, 2019, **163**, 10.
60 L. Gummidi, N. Kerru, O. Ebenezer, P. Awolade, O. Sanni, M. S. Islam and P. Singh, *Bioorg. Chem.*, 2021, **115**, 105210.
61 E. Nezhawy, O. H. Ahmed, M. M. Ramla, N. M. Khalifa and M. M. Abdulla, *Monatsh. Chem.*, 2009, **140**, 531.
62 S. Ramachandran, B. V. Cheriyan and M. V. Aanandhi, *Res. J. Pharm. Technol.*, 2021, **14**, 4513.
63 P. Shukla, M. Singh, V. K. Rai and A. Rai, *New J. Chem.*, 2022, **46**, 3297.
64 M. Isaoglu and N. Cesur, *Anatol. J. Bio.*, 2020, **1**, 22.
65 S. Kalhor, M. Yarie, M. Rezaeivala and M. A. Zolfigol, *Res. Chem. Intermed.*, 2019, **45**, 3453.
66 (*a*) M. A. Zolfigol, M. Navazeni, M. Yarie and R. Ayazi-Nasrabadi, *Appl. Organomet. Chem.*, 2017, **31**, e3633; (*b*) M. A. Zolfigol, M. Navazeni, M. Yarie and R. Ayazi-Nasrabadi, *Res. Chem. Intermed.*, 2018, **44**, 191; (*c*) M. A. Zolfigol, M. Navazeni, M. Yarie and R. Ayazi-Nasrabadi, *RSC Adv.*, 2016, **6**, 92862; (*d*) M. Torabi, M. Yarie and M. A. Zolfigol, *Appl. Organomet. Chem.*, 2019, **33**, e4933.
67 A. Srivastava, P. Singh, M. Gupta, M. S. Ansari, A. Mandhani, R. Kapoor, A. Kumar and D. Dubey, *Urol. Int.*, 2008, **80**, 306.
68 H. X. Pang, Y. H. Hui, K. Fan, X. J. Xing, Y. Wu, J. H. Yang, W. Shi and Z. F. Xie, *Chin. Chem. Lett.*, 2016, **27**, 335.
69 J. Safaei-Ghomi, S. H. Nazemzadeh and H. Shahbazi-Alavi, *Z. Naturforsch., B: J. Chem. Sci.*, 2017, **72**, 927.
70 M. Mohammadi and A. Ghorbani-Choghamarani, *RSC Adv.*, 2022, **12**, 2770.
71 M. Nasr-Esfahani, S. J. Hoseini, M. Montazerozohori, R. Mehrabi and H. Nasrabadi, *J. Mol. Catal. A: Chem.*, 2014, **382**, 99.
72 (*a*) I. V. Alabugin, L. Kuhn, M. G. Medvedev, N. V. Krivoshchapov, V. A. Vil, I. A. Yaremenko, P. Mehaffy, M. Yarie, A. O. Terent'ev and M. A. Zolfigol, *Chem. Soc. Rev.*, 2021, **50**, 10253; (*b*) I. V. Alabugin, L. Kuhn, N. V. Krivoshchapov, P. Mehaffy and M. G. Medvedev, *Chem. Soc. Rev.*, 2021, **50**, 10212; (*c*) M. Torabi, M. A. Zolfigol, M. Yarie and Y. Gu, *Mol. Catal.*, 2021, **516**, 111959; (*d*) M. Torabi, M. Yarie, M. A. Zolfigol, S. Azizian and Y. Gu, *RSC Adv.*, 2022, **12**, 8804.